View metadata, citation and similar papers at core.ac.uk

brought to you by CORE

provided by IntechOpen

We are IntechOpen, the world's leading publisher of Open Access books Built by scientists, for scientists

4,800
Open access books available

122,000
International authors and editors

135M
Downloads

Our authors are among the

154
Countries delivered to

TOP 1%
most cited scientists

12.2%
Contributors from top 500 universities

CLARIVATE ANALYTICS BOOK CITATION INDEX INDEXED

WEB OF SCIENCE™

Selection of our books indexed in the Book Citation Index in Web of Science™ Core Collection (BKCI)

Interested in publishing with us?
Contact book.department@intechopen.com

Numbers displayed above are based on latest data collected.
For more information visit www.intechopen.com

6

Influence of Dissolved Hydrogen on Stress Corrosion Cracking Susceptibility of Nickel Based Weld Alloy 182

Luciana Iglésias Lourenço Lima, Mônica Maria de Abreu Mendonça Schvartzman, Marco Antônio Dutra Quinan, Célia de Araújo Figueiredo and Wagner Reis da Costa Campos
Nuclear Technology Development Centre- CDTN/CNEN
Brazil

1. Introduction

Nuclear power stations are electrical energy stations that use nuclear fission reaction as a source of heat to produce energy. Most of the world's nuclear steam supply systems for generating electricity are based on water cooled and moderated systems of which the most commom design are the Ligth Water Reactors (LWR) varieties: Pressurized Water Reactor (PWR) and the Boiling Water Reactor (BWR). In the construction of these reactors nickel-based alloy 600 and its associated alloys 82 and 182 weld metals were initially selected because of their ability to withstand a variety of severe operating conditions involving corrosive environment, high temperatures, high stresses, and combinations thereof (Gomez-Briceño & Serrano, 2005, Peng, et al., 2007).

Alloy 82 and 182 weld metals are widely used to join austenitic stainless steel to low alloy steel components of PWRs. However, after many years of plant operation, those materials showed susceptibility to stress corrosion cracking (SCC). Since 1994, cracks and leaks have been discovered in about 300 welds of nickel-based alloys 82 and 182 at different PWR plant primary coolant system locations (Scott, 2004, Scott & Meunier, 2007).

Despite many studies have been performed on the SCC behavior of nickel-based alloys the mechanisms are still not well understood. It was observed that the variables that influence the SCC susceptibility of alloy 182 weld metal are quite similar to those associated for nickel-based alloy 600 such as cold work, alloy metallurgical factors, applied or residual stresses, and environmental factors including primary water hydrogen partial pressure, water temperature and chemistry, (Rebak & Szklarska-Smialowska, 1996, Rebak & Hua, 2004).

Actions to mitigate the SCC have been undertaken comprising changes in the chemical environment (optimizing dissolved hydrogen levels, zinc addition and noble metal chemical addition). The use of water chemistry optimization is attractive because many or all components can benefit. In view of the successful application of water chemistry on SCC mitigation in BWR reactors and its system wide benefit, mitigation by adjusting the primary water chemistry in PWR reactors has being considered (Andresen, et al., 2005).

Hydrogen gas is added to the primary circuit coolant at concentrations usually ranging between 25 and 50 cm^3 $H_2.kg^{-1}$ H_2O at standard temperature and pressure (STP). This concentration range is sufficient to inhibit radiolysis of water and thereby minimize corrosion of structural materials (Garbett, et al., 2000, Lima et al., 2011). Besides this, dissolved hydrogen (DH) might affect the SCC behavior of nickel-based alloys. Many experimental studies (Morton et al., 1999, Totsuka, et al., 2000, Attanasio & Morton, 2003) have indicated that the crack growth rate varies with the DH concentration at a given temperature.

In this chapter it is proposed to present the initial results of an evaluation of the dissolved hydrogen influence on the SCC susceptibility of the nickel-based weld alloy 182 using slow strain rate tensile tests (SSRT) conducted at Nuclear Technology Development Centre – CDTN/CNEN.

1.1 Dissimilar metal Weld in pressurized water reactors

A weld between different metals is known as dissimilar metal weld (DMW) and is used in western LWR plants. In Westinghouse and French nuclear power plants design the most important application of this type of weld is between low alloy steel nozzles to austenitic stainless steel pipelines. Typical locations are J-groove welds of nickel alloy 600 vessel head penetrations, pressurizer penetrations and instrument nozzles. In addition, they are used in butt welds in RPV and steam generator inlet and outlet nozzles, pressurizer surge line, safety and relief valve nozzles (Figure 1) (Banford & Hall, 2003, King, 2005, Seifert, et al., 2008).

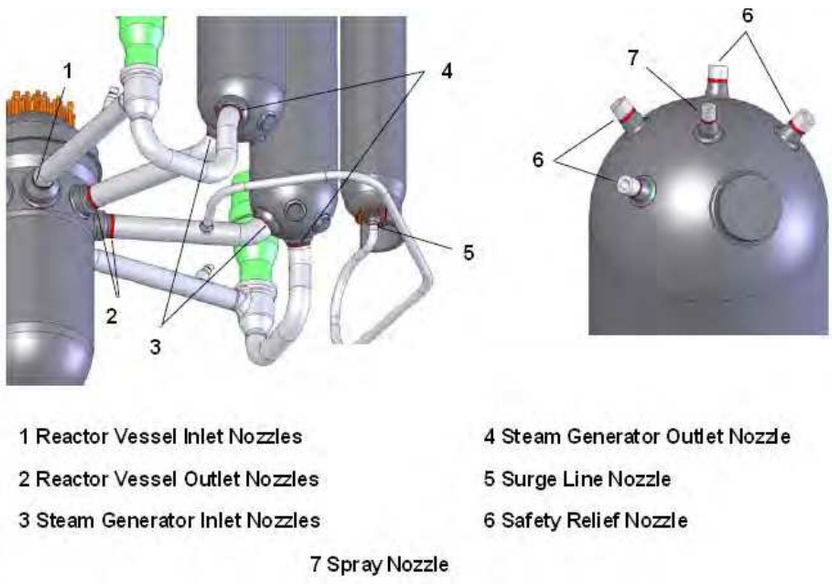

Fig. 1. Alloy 82 and 182 butt welds locations in PWR Westinghouse design plants (King, 2005).

The type and characteristics of the DMW depend on a range of factors; including the specific reactor design, the welding procedure and the weld material (International Atomic Energy Agency [IAEA], 2003, Jang et al., 2008). The welding of two different materials may occur directly, after applying a buttering layer in one of them or by using a transition piece, also

called safe end, between the two dissimilar materials (Figure 2). Nickel-based alloy 82 or 182 is generally used as weld metal material in the buttering layer and in the J-groove weld (IAEA, 2003, Miteva & Taylor, 2006).

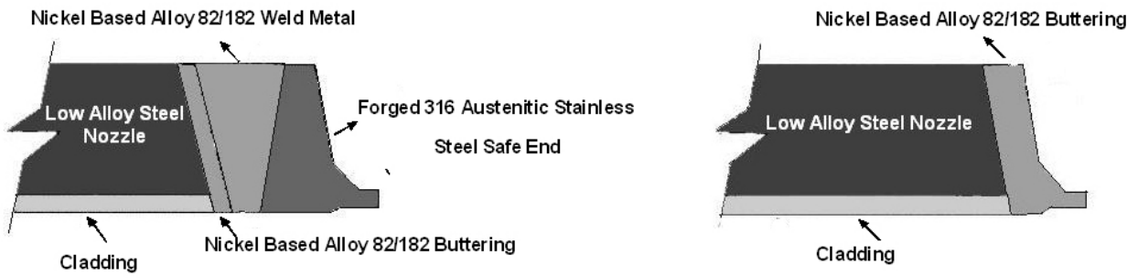

Fig. 2. Dissimilar metal weld variations of the Westinghouse plant design, (a) weld with a safe end and (b) weld without a safe end (Miteva & Taylor, 2006).

The use of safe end avoids making of DMW on site, during the component installation in the nuclear power plant. The transition piece is welded to low alloy steel nozzles in the manufacturer´s shop under controlled conditions, so the subsequent weld to connect the component is a conventional similar weld that can be made on site. The use of the buttering layer is an alternative way to accommodate the differences in the composition and properties of the two base metals, such as the melting point, coefficient of thermal expansion and to make difficult the migration of undesirable alloying elements from base metal to weld metal. Buttering can also be used to alleviate the requirements of postweld heat-treatment (PWHT) (King, 2005, Davis, 2006).

In the Westinghouse plant design the dissimilar metal welds are made in three steps. In the first stage a buttering layer is applied to the low alloy steel with a final thickness varying between 5 and 8 mm. The layer is applied by gas tungsten arc process (GTAW) with nickel-based alloy 82 and 182 as weld metal. The second stage consists of the stress relief heat treatment and the machining of the buttered surface to obtain the weld edges. The temperature and the duration of the heat treatment depend on the thickness of the low alloy steel component and the number of buttering layers. Usually the stress relief heat treatment is undertaken at temperatures from 580ºC. In the third stage the buttered low alloy steel is welded to austenitic stainless steel by the GTAW process with nickel-based alloy 82 for the root pass. The joint is completed with nickel-based alloy 182, using the shielded metal arc process (SMAW) (Fallatah et al., 2002, Miteva & Taylor, 2006).

The use of pre-heating is recommended for materials with a high level of carbon equivalent and components of high thickness. Pre-heating encourages a decrease in the cooling speed, which reduces the likelihood of martensite forming in the heat affected zone (HAZ) of the low alloy steel and reduces the occurrence of hot cracking in the materials involved. Heat treatment after welding may or may not take place (Schaefer, 1979, Kou, 2003, Miteva & Taylor, 2006).

1.2 Stress corrosion cracking in pressurized water reactors

Environmentally assisted cracking (EAC) in the form of stress corrosion cracking (SCC) is one of the most critical kinds of damage experienced in nuclear power plants. It is a potentially critical issue concerning safety of plant operation and plant life extension (American Society of Metals [ASM], 2006). SCC phenomenon consists of a degradation process resulting from a combined and synergistic interaction of aggressive environment, tensile stresses and susceptible material, as well as the time for the phenomenon to occur. This phenomenon has been reported in dissimilar metal welds in various nuclear power plants all over the world. Various studies carried out since the 1980s have demonstrated that nickel-based alloys 82 and 182 are susceptible to the SCC phenomenon (Andresen et al., 2002, Fukumura & Totsuka, 2010). In the end of the year 2000, three PWRs experienced cracking concerned to dissimilar metal welds between the main austenitic stainless steel primary circuit piping and the outlet pressure vessel nozzles, believed to be stress corrosion cracking, of major primary circuit welds made from nickel-based alloy 82 or 182. (Pathania et al., 2002 Amzallag et al., 2002, Banford & Hall, 2005, Alexandreanu et al., 2007).

In the case of susceptible material the main factors that influence the SCC susceptibility of nickel-based alloy 600 and its associated alloys 82 and 182 weld metals are chemical composition, microstructure and heat treatment of the material. The levels of carbon and chromium are important variables when evaluating the chemical composition. Data from laboratories have been demonstrated that the increase of chromium content correlates with decreasing in the SCC susceptibility (White, 2004, White, 2005). The grain size and the presence and location of inclusions and precipitates are also relevant variables in the evaluation of materials susceptibility to this phenomenon. The presence of continuous or semicontinuous chromium carbides at the grain boundaries and the absence of these carbides in the grain matrix tend to increase the resistance of nickel-based alloys to SCC susceptibility. Various models have been proposed to explain this effect, but the reasons for this beneficial effect are not completely understood. (Rebak, et al., 1993, Aguillar et al., 2003, Tsai et al., 2005, Andresen & Hickling, 2007).

Two principal sources of tensile stress are able to cause the SCC phenomenon – the tensile stresses resulting from the operating conditions (pressure, temperature and mechanical load) and the residual stresses resulting from the original fabrication process, such as welding. The tensile stresses that exist during an operation are taken into account when planning nuclear power stations and must comply with the specific standards and codes (American Society of Mechanical Engineering [ASME], 2004). However, high residual stresses may be created during the manufacturing and welding processes. The residual stresses that arise from welding may be higher than the operating stresses and tend to be dominant driving force behind the crack growth. It is the combination of operating condition stresses and residual stresses that lead the occurrence of the SCC phenomenon (Sedricks, 1990, ASM, 1992, Speidel & Magdowski, 2000, Gorman, et al., 2009).

Among all of the factors that affect SCC susceptibility, the effect of environmental conditions is particularly important. The concentrations of oxygen and hydrogen, the corrosion potential, temperature and the pH balance of the solution play an important role

in this process. The SCC phenomenon is a thermally activated process and can be represented by the Arrhenius law. Places which the operating temperatures are high develop cracks more rapidly than regions where the operating temperatures are lower. It has also been observed that crack growth rates of nickel-based alloys and weld metals in simulated PWR primary water environments generally increase with increasing temperature (Nishikawa et al., 2004, Lu et al., 2008, Schvartzman et al., 2009).

1.3 Stress corrosion cracking in pressurized water reactors mitigation process

The mitigation of primary water stress corrosion cracking is defined as a adoption of remedial measures to reduce the frequency and/or to delay the stress corrosion crack initiation and/or propagation. The term mitigation does not mean completely elimination or prevention of the phenomenon, imply only in the control of the variables that affect the SCC susceptibility (Scott; Meunier, 2007).

The metodologies developed to prevent and to mitigate primary water SCC of the nickel-based alloy 600 and its associated alloys 82 and 182 weld metals include:

Materials Replacement: replacement in the new nuclear power plants of nickel-based alloy 600 and alloys 82 and 182 components for materials more resistant to SCC, nickel-based alloy 690 and its associated alloys 52 and 152 weld materials, has been considered. This remedial measure sometimes can be unavoidable in nuclear power plants currently in operation due to the high cost and difficulties in relation to the operation of this modification (security issues due to the high radiation level of the components) (King, 2005).

Surface Treatment: consist in a process that reverse the unfavorable residual stress field, leaving a compressive stresses on the surface. The presence of the compressive stress inhibits initiation and propagation of SCC. Among this method can be cited: weld overlay, induction heating stress improvement and mechanical stress improvement process, (Giannuzzi, et al., 2004).

Water Chemistry Changes: mitigation can be obtained by implementing changes to the operating environment that reduces the material's susceptibility to SCC. Among this method can be cited: addition of zinc, reduction of operating temperature and control of the dissolved hydrogen concentration (Andresen, Hickling, 2007).

In recent years, it became evident that the dissolved hydrogen concentration added to the PWR primary circuit coolant can influence the nickel-based alloy stress corrosion cracking susceptibility by changing the thermodynamic equilibrium of nickel oxide (NiO) phase formation (Morton et al., 2001, Takiguchi et al., 2004). Given the fact that the corrosion potential of nickel-based alloys in deareted water is controlled by the H_2/H_2O reaction, which represents two related reactions: oxidation ($2H^+ + 2e^- \leftrightarrow H_2$) and reduction ($H_2 + 2OH^- \leftrightarrow 2H_2O + 2e$), and the line that representing this reaction is parallel to the metal/metal oxide (Ni/NiO) phase boundary (Figure 3) variations in the dissolved hydrogen concentrations can shift the corrosion potential making that this potential reach values close to the Ni/NiO phase transition (Attanasio & Morton, 2003, Andresen et al., 2008).

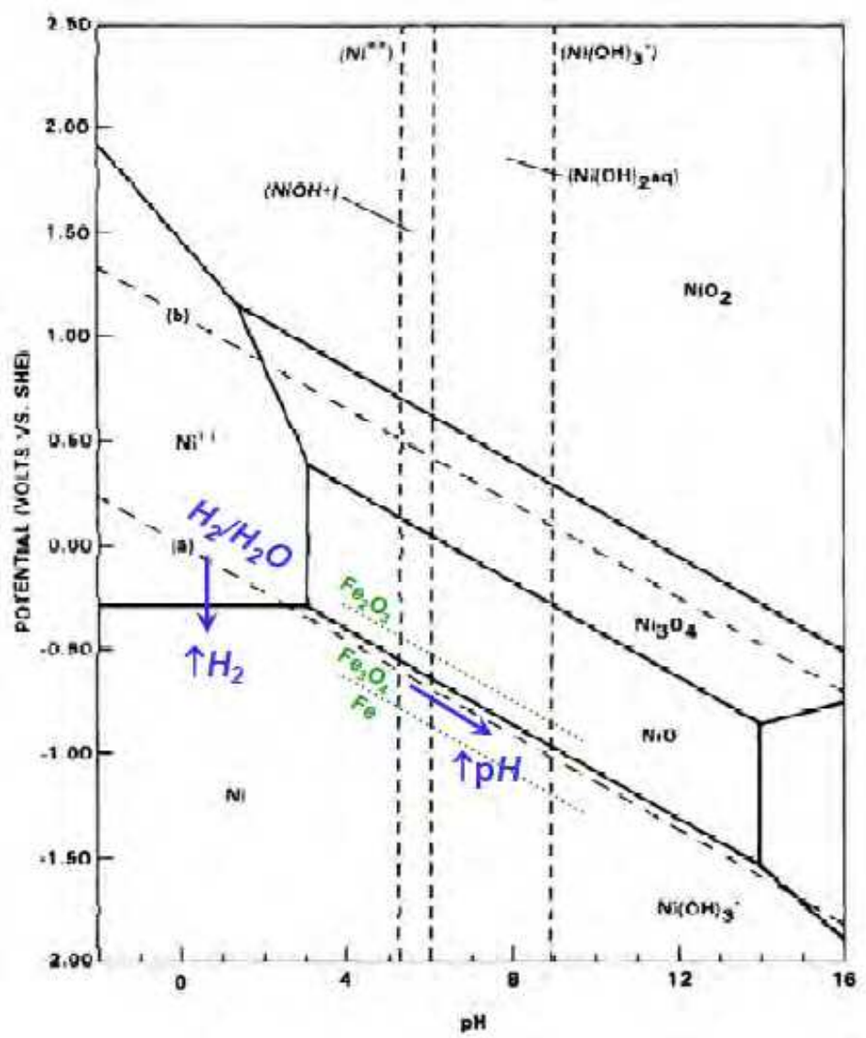

Fig. 3. System Ni – H_2O Pourbaix Diagram at 300°C (Andresen, et al., 2008).

Testing conducted by Attanasio and Morton (Attanasio & Morton, 2003) at various aqueous DH levels and temperatures has shown that a maximum in crack growth rate (CGR) occurs for nickel-based alloys in proximity to the Ni/NiO phase transition. Because the Ni/NiO boundary change with temperature the hydrogen level required to transit Ni/NiO boundary is not fixed. For nickel alloys at 325°C the peak in crack growth rate occurs at a hydrogen content of about 10 cm^3 H_2 (STP).kg^{-1} H_2O. As hydrogen concentration is increased from low values the growth rate begins to increase and then decrease, as shown schematically in Figure 4 (Andresen et al., 2005, Andresen et al., 2008).

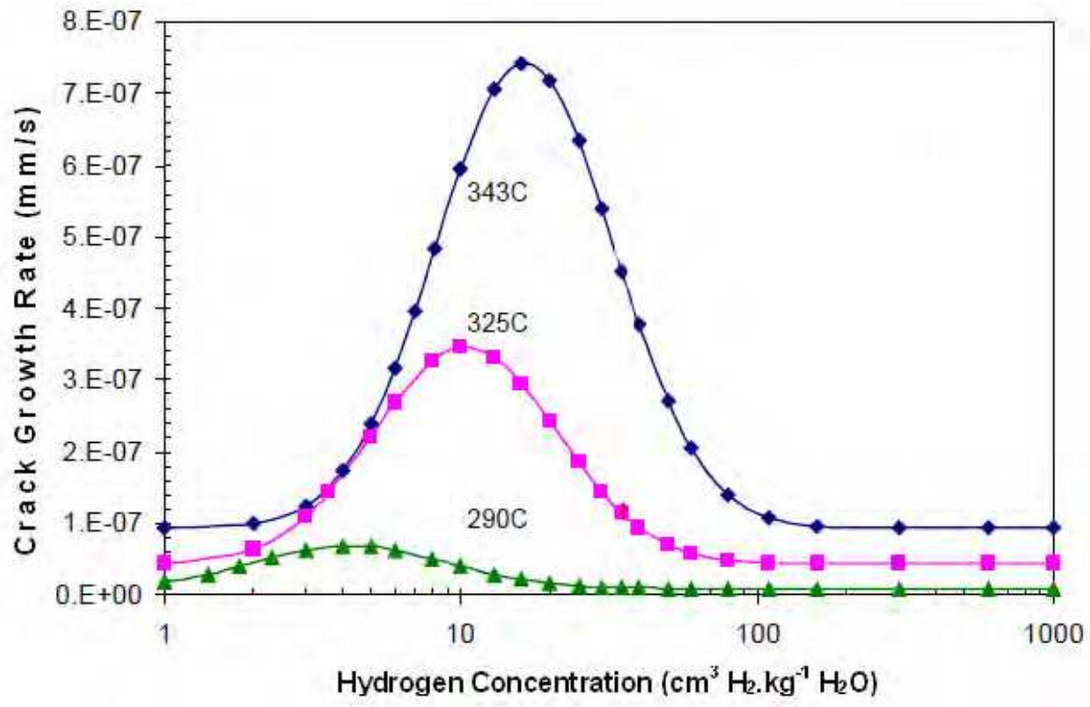

Fig. 4. Predicted effect of hydrogen concentration on the nickel-based alloys crack growth rate (Andresen et al., 2008).

Although many laboratory studies have been performed, the mechanistic basis for the effect of the primary water dissolved hydrogen on the susceptibility of nickel based alloys to SCC is still not yet completely understood.

2. Effect of dissolved hydrogen on stress corrosion cracking of nickel weld alloy 182

2.1 Experimental

The alloy 182 material was retrieved from a J groove weld joint that was made by joining two thick plates (ASTM A-508 class 3 – 130 x 300 x 36 mm and AISI 316L – 130 x 300 x 31 mm) with alloy 182, thus forming a dissimilar metal weld. The two base metals were used as received, AISI 316L in the rolled condition and ASTM A-508 class 3 in the forged condition. Five passes of buttering were applied on the ASTM A-508 class 3 plate by Gas Tungsten Arc Welding (GTAW) with Alloy 82 wire (AWS A5.14 ENiCr-3). The thickness of the buttering layer was about 8 mm. A chamfer was machined on the buttered side and the plate was subjected to a post weld heat treatment at 600°C for 2 hours to relieve the residual stresses. The final weld joint was produced by three root passes by GTAW with alloy 82 filler and thirty-seven weld passes by Shielded Metal Arc Welding (SMAW) with an alloy 182 shielded electrode (A5.11 ENiCrFe-3). The chemical composition of both base metals and filler wires is shown in Table 1. Figure 5 shows the microstructure of the alloy 182 weld joint.

	C	Mn	Si	P	S	Cr	Ni	Nb	Ti	Mo
316L	0.023	1.46	0.48	0.02	0.003	16.7	9.8	0.02	0.03	2.10
A508	0.21	1.34	0.23	0.005	0.003	0.09	0.68	0.002	0.001	0.51
182	0.05	6.16	0.34	0.01	0.009	14.3	70.3	2.07	0.05	0.24
82	0.04	3.4	0.14	0.01	0.005	18.9	73	2.47	0.25	0.16

Table 1. Chemical composition of the base and filler metals (wt%). (Fe – Bal.)

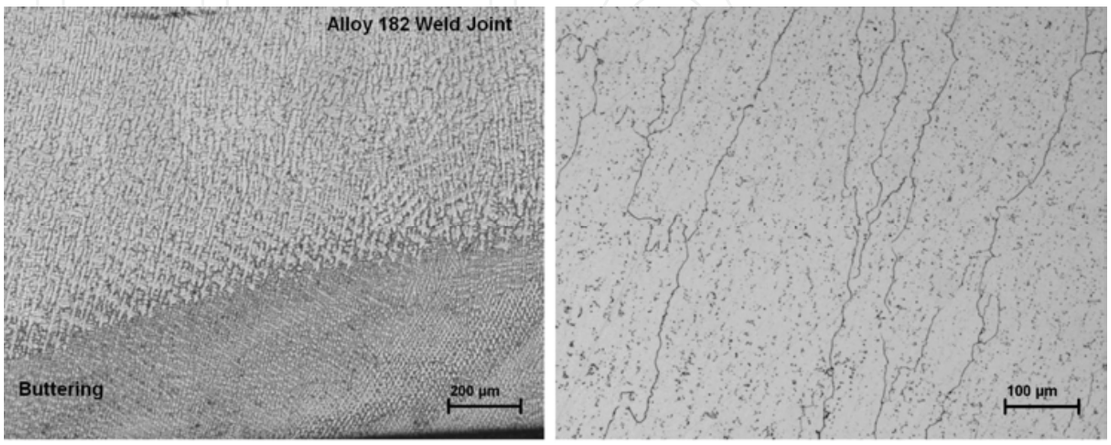

Fig. 5. Microstructure of Alloy 182 weld joint.

The finished weld joint (from now on referred to as Alloy 182 weld) was not heat-treated. It was submitted to nondestructive tests such as dye penetrant and radiographic tests, and no weld defects were revealed. Figure 6 shows a schematic of the weld design. The key welding parameters are summarized in Table 2.

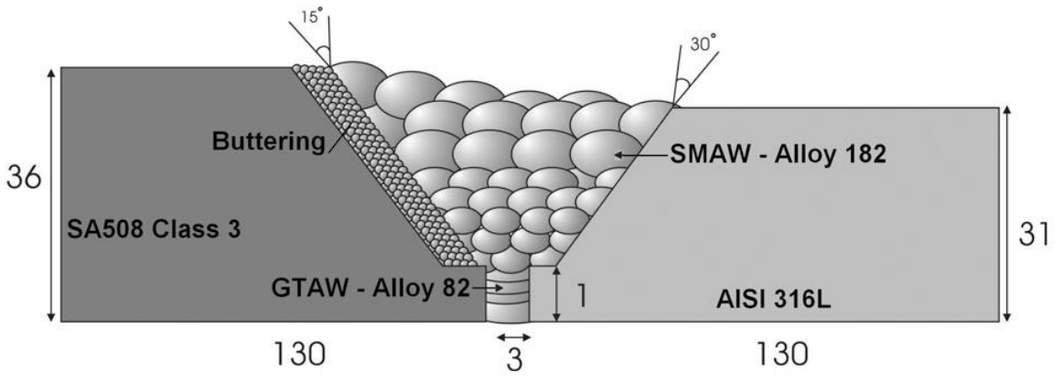

Fig. 6. Schematic of the weld design (dimensions in mm).

Weld Pass	Process	Filler Metal	Electrode Size (mm)	Current (A)	Voltage (V)	Travel Speed (mm/s)
Buttering	GTAW	82	2.5	90 – 130	17.5 – 18	1.8 – 3.0
1 - 3	GTAW	82	2.5	126 – 168	20 – 22	1 – 1.2
4 - 37	SMAW	182	4	– 135	22 – 26	1 – 3.5

Table 2. Welding parameters.

The influence of dissolved hydrogen on SCC susceptibility of the specimens was assessed by means of slow strain rate tensile (SSRT) test. The SSRT tests were carried out in accordance with ASTM G 129-95 standard (ASTM [American Society for Testing and Materials], 1995). The applied strain rate was $3x10^{-7}$ s^{-1}, which is an adequate strain rate to promote SCC of Alloy 182 weld in PWR primary water environments (Totsuka et al., 2003).

Specimens for the stress corrosion tests were taken from the Alloy 182 weld in the longitudinal direction using electro discharge machining (EDM). They were machined into tensile specimens with 25 mm gauge length and 4 mm gauge diameter (Figure 5), in conformity with ASTM G49-2000 and ASTM E8-2000 standards (ASTM, 2000a, ASTM, 2000b). Prior to the test, the specimens gauge length surface was polished with # 2000 silicon carbide (SiC) paper, degreased with acetone in an ultrasonic cleaner, washed with distilled water and finally dried in air. All the tests were performed at an open circuit potential (E_{OCP}) and the specimens were exposed to the environment for at least 24 hours (h) before applying load to stabilize the surface oxide layer. Three testing were performed for each condition studied.

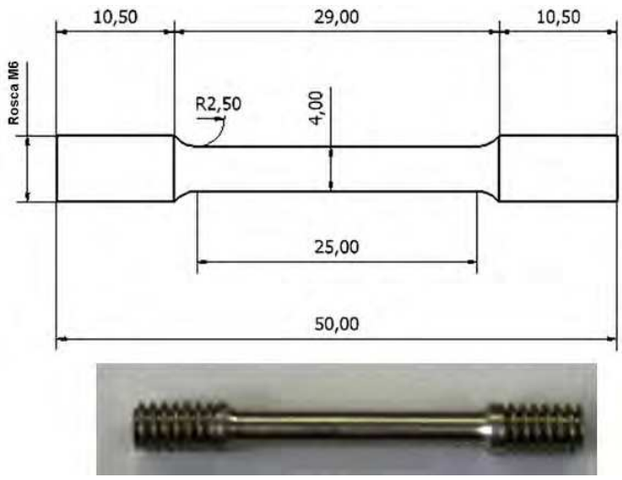

Fig. 7. Slow Strain Rate Test specimen (dimensions in mm).

The specimens were tested in simulated beginning-of-cycle PWR primary coolant environment (1000 ppm B as boric acid and 2 ppm Li as lithium hydroxide) at temperature of 325°C and pressure of 12.5 MPa. Deionized water and analytical grade reagents were used. The test solution pH and conductivity at room temperature were 6.5 and 21 $\mu S.cm^{-1}$, respectively. The dissolved oxygen (DO) concentration was less than 5 ppb oxygen and it was obtained by bubbling pure nitrogen gas (N_2) in the work tank. After the DO content was < 5 ppb, the desired DH level were adjusted by bubbling hydrogen gas (H_2). Tests were carried out at the levels of dissolved hydrogen of 2, 10, 25 and 50 cm^3 H_2 (STP).kg^{-1} H_2O.

The SCC tests were conducted in 1.5 L type AISI 321 stainless steel autoclave, with a high temperature water circulation system. The facility was designed for SCC testing in simulated PWR or BWR environments. It is equipped with a servohydraulic loading system controlled by displacement or load. The displacement is measured by a linear variable differential transformer (LVDT) and the load is measured by a load cell. The autoclave is heated externally by an electric oven controlled continually by a proportional-integral-

differential (PID) system. During the execution of the tests, on-line measurements of load, displacement, temperature, pressure, conductivity and oxygen concentration are taken. A software application developed in the LabVIEW environment is responsible for acquiring the data and for their graphic representation. Figure 8 shows a photo of the installation.

Fig. 8. Photo of the installation of SCC tests.

The susceptibility to SCC was evaluated by means of the ductility parameters obtained from the stress-strain curves and the fracture surface analyses. The fracture surfaces of the samples were examined using scanning electron microscope (SEM). All results were compared to baseline tests conducted in inert medium (N_2 – nitrogen gas) at the same strain rate. The ratio of time to failure at test condition to baseline ($t_{fsolution}/t_{fN2}$) and the ratio of elongation at test condition to baseline ($\varepsilon_{solution}/\varepsilon_{N2}$) were used as parameters to measure the degree of SCC susceptibility. In general, ratios near 100 indicate higher ductility and less susceptibility to SCC (ASTM, 1995, Nace [National Association of Corrosion Engineers], 2004).

The SCC susceptibility was also estimated using SSRT crack growth rate, which is defined as:

$$\text{SSRT crack growth rate} = \text{Crack length} \times \text{SCC fracture ratio} \div \text{fracture time} \quad (1)$$

The influence of dissolved hydrogen on Alloy 182 weld stress corrosion cracking behavior was also studied using electrochemical technique. For this purpose, open circuit potential (E_{OCP}) versus time measurements were performed in 325°C simulated PWR chemistry at hydrogen levels of 2, 10, 25 and 50 cm^3 (STP) $H_2.kg^{-1}$ H_2O. Specimens were cut from the Alloy 182 weld in the longitudinal direction using electro discharge machining (EDM). They were machined into cylindrical specimens (5 mm diameter and 10 mm length) were mechanically ground to a surface finishing equivalent to # 600 SiC paper.

The open circuit potential (E_{OCP}) was measured after about 500 h of exposure. Measurements were conducted in a conventional three electrode cell. The electrochemical composition consisted of the working electrode, an yttrium stabilized zirconia (YSZ) electrode filled with a mixture of Ni/NiO powder and a platinum counter electrode (Figure 9). A conversion factor of – 0.800 mV taken from Bosch´s work (Bosch et al., 2003) for the temperature an pH conditions of the test was used to convert the measured values to hydrogen electrode potential values (V_{SHE}). The measurements were performed using a potentiostat system.

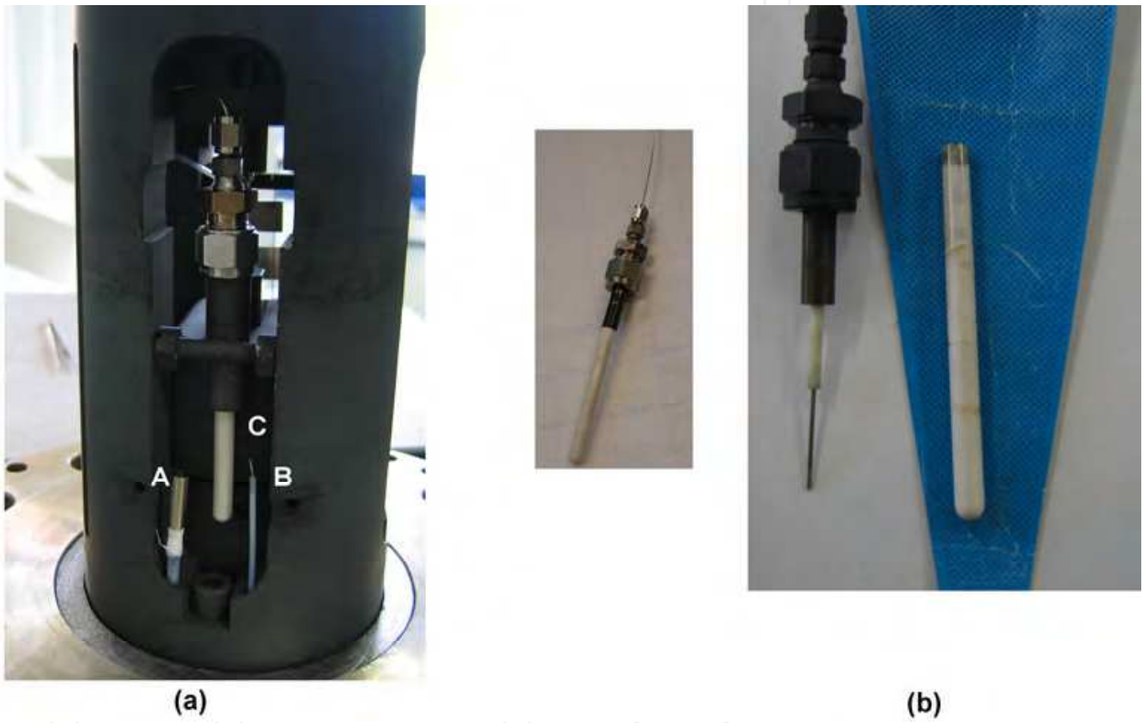

Fig. 9. (a) Electrodes disposition in autoclave, A: work electrode, B: platinum counter electrode, C: yttrium stabilized zirconia (YSZ) reference electrode and (b) detail of yttrium stabilized zirconia (YSZ) reference electrode.

2.2 Results and discussion

The open circuit potential measurements results of Alloy 182 weld in 325ºC simulated PWR chemistry at hydrogen levels of 2, 10, 25 and 50 cm^3 (STP) $H_2.kg^{-1}$ H_2O are given in Figure 10. It is important to note that at 10 cm^3 (STP) $H_2.kg^{-1}$ H_2O the potential took a longer time to stabilize, the E_{OCP} was considered stabilized when no significant variation was observed.

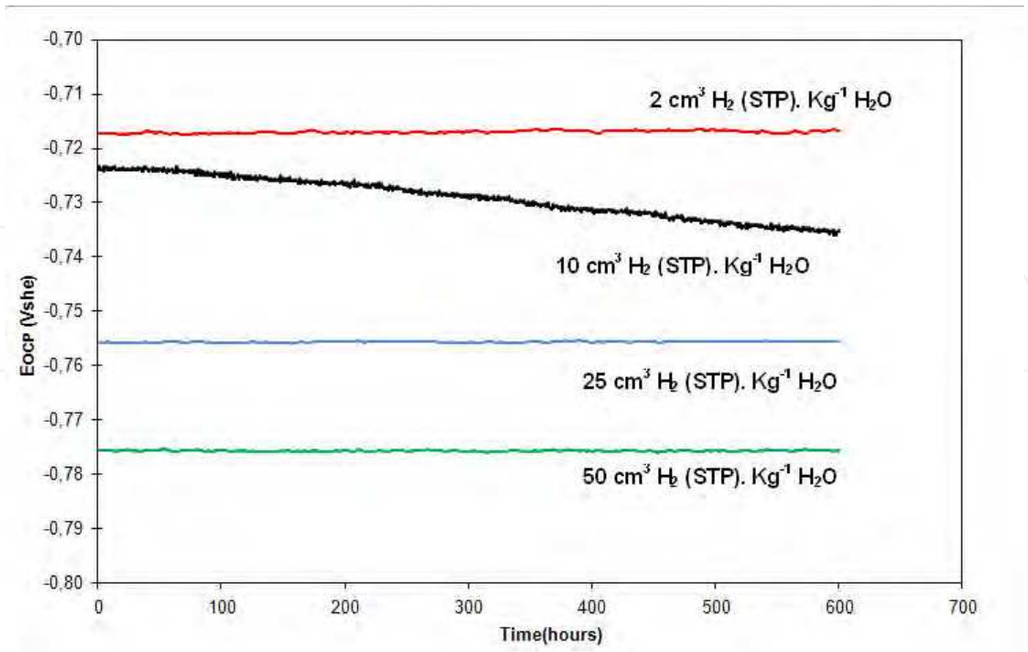

Fig. 10. OCP measurements of Alloy 182 weld in 325ºC simulated PWR chemistry at hydrogen levels of 2, 10, 25 and 50 cm^3 (STP) $H_2.kg^{-1}$ H_2O.

Figure 11 (a) shows the E_{OCP} x pH diagram of nickel at 300ºC in pure water obtained from EPRI´s report (Andresen & Hickling, 2007) and Figure 11 (b) shows the relationship between the corresponding E_{OCP} values obtained in this work for Alloy 182 weld in PWR environment as a function of the test solution pH (pH = 7) and the dissolved hydrogen level.

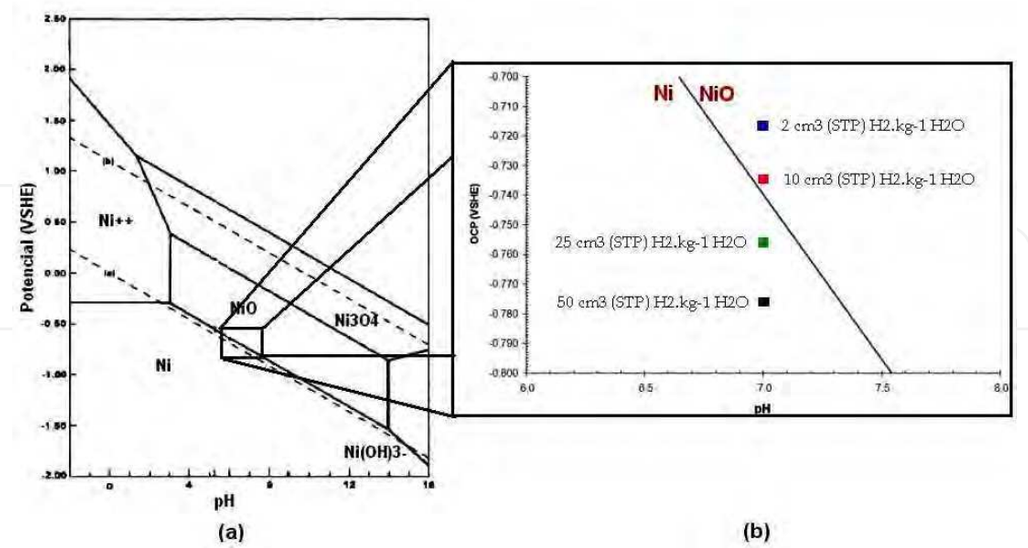

Fig. 11. (a) Potential x pH diagram of nickel at 300ºC in pure water (Andresen & Hickling, 2007), (b) detail of the corresponding E_{OCP} values obtained for Alloy 182 weld in PWR environment to the line of Ni/NiO transition as a function of the pH of test solution (pH-7) and the dissolved hydrogen level.

It is observed that at 10 cm^3 H_2 (STP).kg^{-1} H_2O the potential is closer to the Ni/NiO phase transition and at 50 cm^3 H_2 (STP).kg^{-1} H_2O the potential is far away. Studies conducted for the nickel based alloys 600 and X-750 in pure water have shown that the influence of dissolved hydrogen on the SCC susceptibility may be related by the extent that the corrosion potential deviates from of the potential that corresponds to the transition of Ni/NiO ($\Delta ECP_{Ni/NiO}$). A maximum in SCC susceptibility is observed in a narrow region near the Ni/NiO phase transition (Totsuka et al., 2002, Attanasio & Morton, 2003, Andresen et al., 2008).

Table 3 shows the values of $\Delta ECP_{Ni/NiO}$ obtained in PWR solution at 325°C and concentrations of dissolved hydrogen of 2, 10, 25 and 50 cm^3 H_2 (STP).kg^{-1} H_2O. In this table the value of $\Delta ECP_{Ni/NiO}$ for 10 cm^3 H_2 (STP).kg^{-1} H_2O was considered zero because of the proximity of the transition line Ni/NiO. The present result is in accordance with the thermodynamic model proposed by Attanasio and Morton (Attanasio & Morton, 2003). According to this model the concentration of DH at 325°C, which corresponds to this transition, is approximately 10 cm^3 H_2 (STP).kg^{-1} H_2O.

Test Enviroment	E_{OCP} (mV_{SHE})	$\Delta ECP_{Ni/NiO}$ (mV_{SHE})
2(1)	-717	-18
10(1)	-735	0
25(1)	-756	21
50(1)	-776	41

Table 3. E_{OCP} and $\Delta ECP_{Ni/NiO}$ values obtained for Alloy 182 weld in PWR environment at 325°C as a function of the pH of test solution (pH-7) and the dissolved hydrogen level. (1) cm^3 H_2 (STP)/kg H_2O.

The stress-strain curves obtained from SSRT for Alloy 182 weld in the DH levels and in the baseline conditions are presented in Figure 12. Table 4 summarizes the mechanical properties and Table 5 shows the results of time to failure ratio and elongation ratio of the specimens under the five different environments.

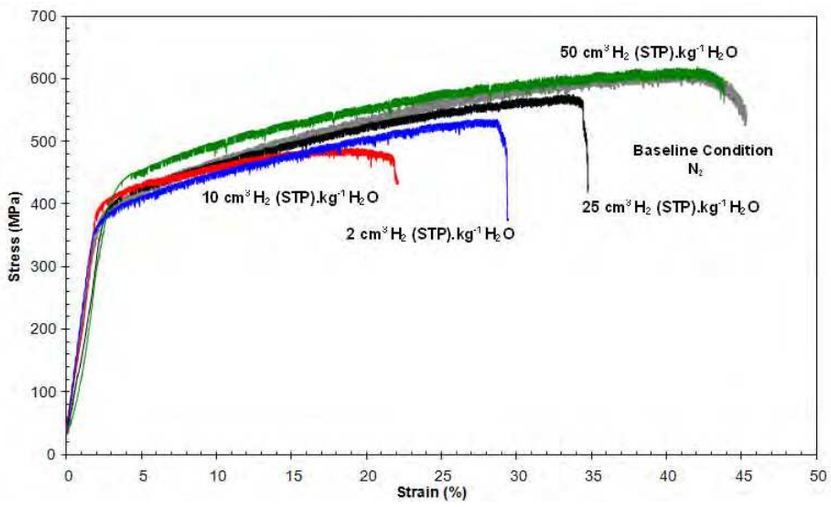

Fig. 12. Stress - Strain curves of Alloy182 weld obtained from SSRT at 325° C, at strain rate of $3x10^{-7}$ s^{-1} in PWR primary water condition with 2, 10, 25 and 50 cm^3 H_2 (STP).kg^{-1} H_2O and baseline (N_2 gas).

Test Environment	Yield Strength (MPa)		Ultimate Tensile Strength UTS (MPa)		Plastic Strain to Failure E (%)	
	Range	Mean	Range	Mean	Range	Mean
Baseline N_2 (gas)	347 - 399	375	610 - 616	612	40 – 45	42
2(1)	385 - 391	388	537 – 575	557	34 - 36	35
10(1)	380 - 390	385	490 – 547	507	20 - 22	21
25(1)	345 - 391	368	524 - 536	530	29 - 32	28
50(1)	380 - 416	398	605 - 618	610	40 -44	42

Table 4. Mechanical Properties obtained from SSRT test at 325ºC. (1) cm^3 H_2 (STP)/kg H_2O.

Test Environment	Time to Failure (Hours)		$T_{f\ solution}/T_{f\ N2}$ (%)	$E_{solution}/E_{N2}$ (%)
(1) cm^3 H_2 (STP)/kg H_2O.	Range	Mean		
Baseline N_2 (gas)	367 - 418	391	-	-
2(1)	317 - 336	324	83	83
10(1)	197 - 240	216	55	51
25(1)	266 - 298	278	72	71
50(1)	367 - 401	384	99	100

Table 5. Time to failure and elongation ratios obtained from SSRT test at 325ºC.

Note that at 10 cm^3 H_2 (STP).kg^{-1} H_2O there was a reduction in the resistance limit and ductility of the material, the ultimate tensile strength was 21% lower than the baseline. This reduction was attributed to the SCC process that led to the weakness of the material. It can also be seen that the specimens exposed at 10 cm^3 H_2 (STP).kg^{-1} H_2O presented the elongation and time to failure ratios lower than 100% indicating an effect of the environment on the material behavior and a higher susceptibility to SCC. At 50 cm^3 H_2 (STP).kg^{-1} H_2O these values are close to 100% indicating the lower susceptibility to SCC. Figure 13 shows the SEM micrographs of the fracture surfaces of Alloy 182 weld tested in nitrogen gas at 325°C. The fracture surface was completely ductile with extensive shear parts.

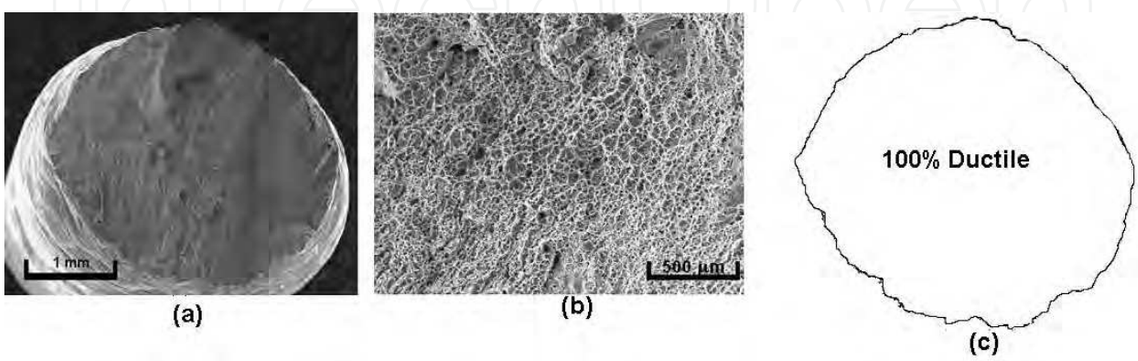

Fig. 13. SEM micrographs of Alloy 182 weld fractured surface tested at 325°C in baseline (N_2 gas) and at strain rate of $3x10^{-7}$ s^{-1} (a) overview (b) detail (c) fraction of fracture.

The respective SEM micrographs of Alloy 182 weld tested at 2, 10 25 and 50 cm^3 H_2 (STP).kg^1 H_2O are shown in Figures 14 to 17. All surfaces exhibit ductile fracture in the middle of the specimen and areas of brittle fracture at the edges, indicating crack initiation by SCC. The fracture mode was intergranular. The intergranular stress corrosion cracking (IGSCC) facets reached an average depth of 836 μm, 1300 μm, 1040 μm and 573 μm for 2, 10, 25 and 50 cm^3 H_2 (STP).kg^{-1} H_2O, respectively. The area of intergranular fracture decreased from 3.33 mm^2 to 0.43 mm^2 when the DH concentration in test solution increased from 10 to 50 cm^3 H_2 (STP).kg^{-1} H_2O. These results are consistent with the stress-strain curves obtained in SSRT, which indicates a higher susceptibility to SCC at 10 cm^3 H_2 (STP).kg^{-1} H_2O.

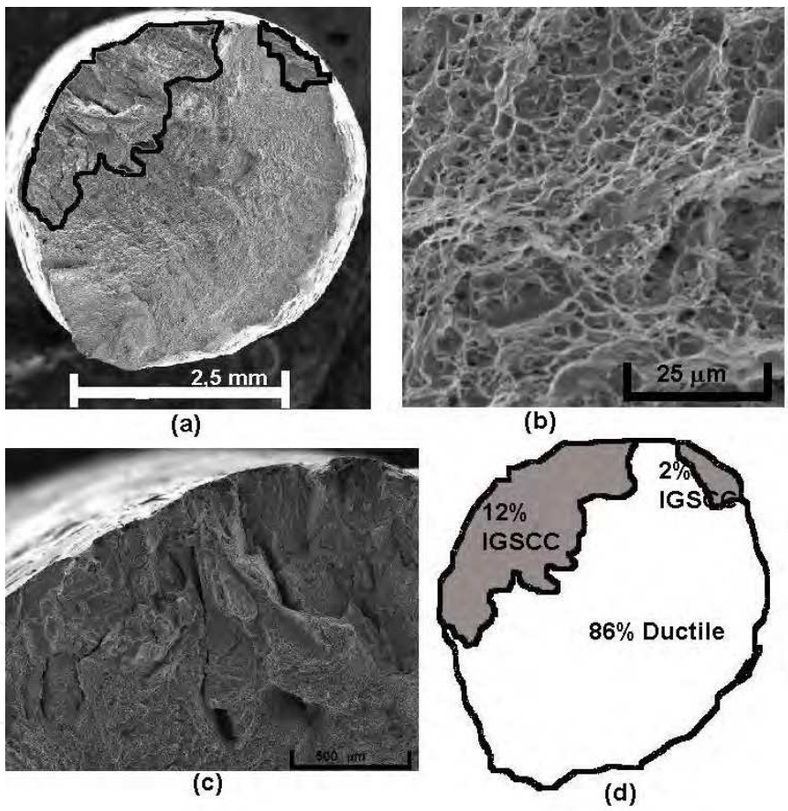

Fig. 14. SEM micrographs of Alloy 182 weld fractured surface of SSRT at 325ºC in PWR primary water with 2 cm^3 H_2 (STP).kg^{-1} H_2O and at strain rate of $3x10^{-7}$ s^{-1} (a) overview (b) detail of ductile fracture (c) detail of IGSCC fracture failure (d) fraction of fracture.

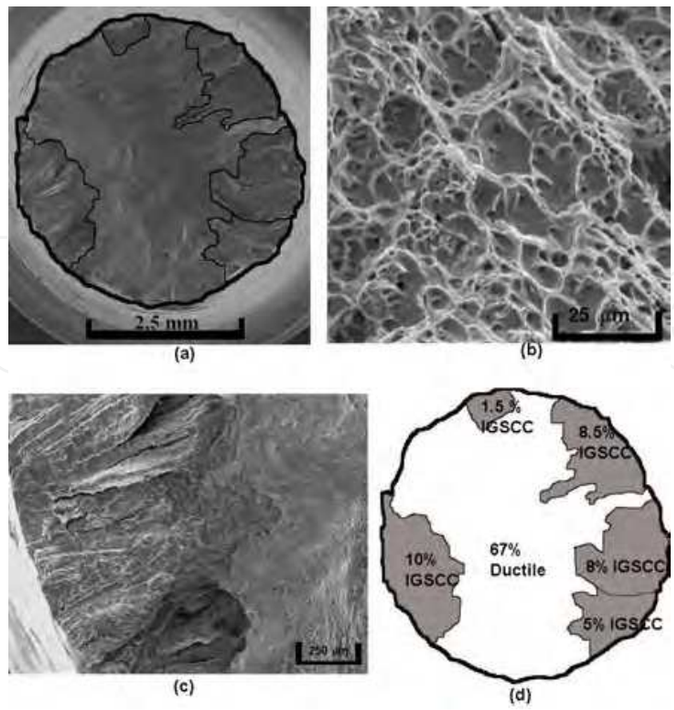

Fig. 15. SEM micrographs of Alloy 182 weld fractured surface of SSRT at 325ºC in PWR primary water with 10 cm^3 H_2 (STP).kg^{-1} H_2O and at strain rate of $3x10^{-7}$ s^{-1} (a) overview (b) detail of ductile fracture (c) detail of IGSCC fracture failure (d) fraction of fracture.

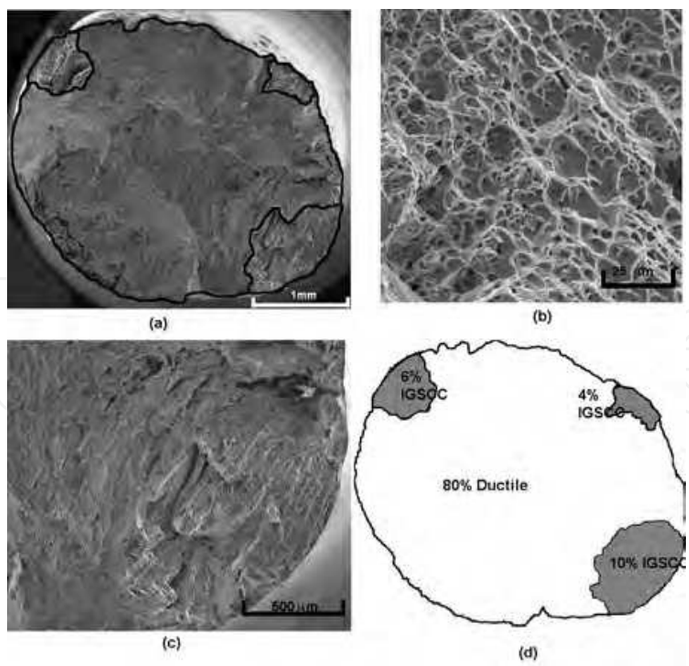

Fig. 16. SEM micrographs of Alloy 182 weld fractured surface of SSRT at 325ºC in PWR primary water with 25 cm^3 H_2 (STP).kg^{-1} H_2O and at strain rate of $3x10^{-7}$ s^{-1} (a) overview (b) detail of ductile fracture (c) detail of IGSCC fracture failure (d) fraction of fracture.

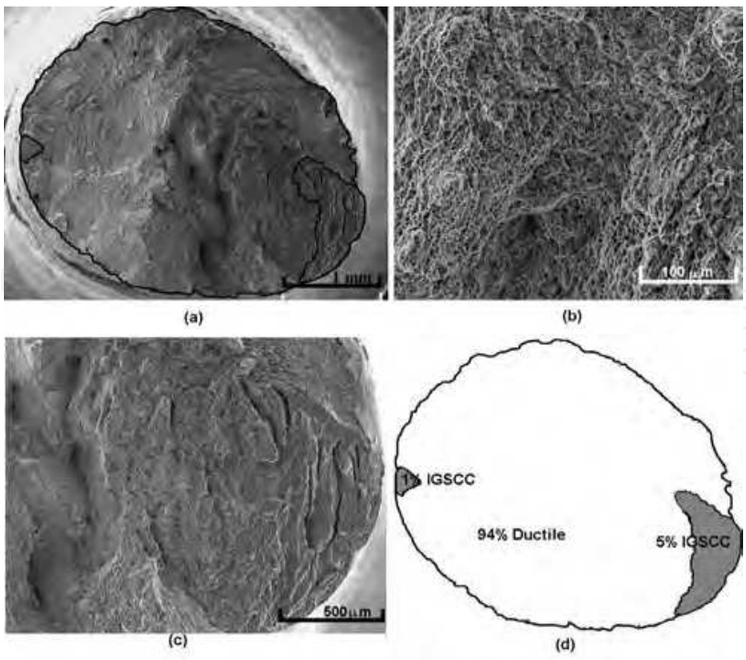

Fig. 17. SEM micrographs of Alloy 182 weld fractured surface of SSRT at 325ºC in PWR primary water with 50 cm^3 H_2 (STP).kg^{-1} H_2O and at strain rate of $3x10^{-7}$ s^{-1} (a) overview (b) detail of ductile fracture (c) detail of IGSCC fracture failure (d) fraction of fracture.

As shown in Figure 18, extensive secondary cracks in the gauge section were observed in the sample that was exposed to 10 cm^3 H_2 (STP).kg^{-1} H_2O in direct contrast with the absence of secondary cracking observed at 50 cm^3 H_2 (STP).kg^{-1} H_2O. According to Brown and Mills (Brown & Mills, 2003) the presence of secondary cracks on the gauge sections of the test samples are also indicative of the weakness of the material attributed to the SCC process, also indicating increased SCC susceptibility of Alloy 182 weld at 10 cm^3 H_2 (STP).kg^{-1} H_2O.

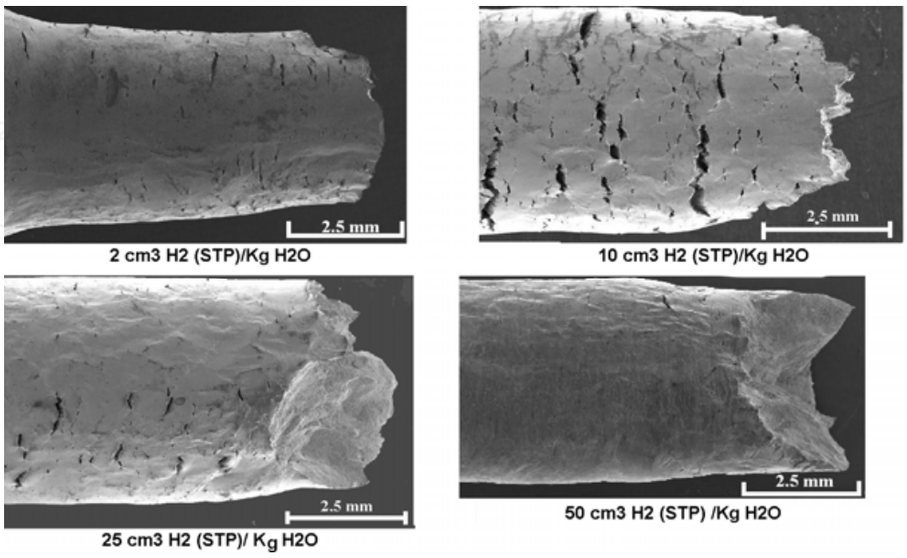

Fig. 18. Gauge section of the specimens tested in the four different environments.

Table 6 shows a summary of the crack growth rate for the four DH conditions calculated using Equation (1) and Figure 19 shows the relationship between dissolved hydrogen and crack growth rate obtained for concentrations of 2, 10, 25 and 50 cm^3 H_2 (STP).kg^{-1} H_2O.

DH cm^3 H_2 (STP) /kg H_2O	Deepest Crack (mm)	A_{IGSCC} (%)	$T_{failure}$ (h)	Crack Growth Rate (mm/s)
2	0.84	14	324	$1{,}3x10^{-7}$
10	1.30	33	216	$5{,}0x10^{-7}$
25	1.04	20	278	2.1×10^{-7}
50	0.57	6	384	2.9×10^{-8}

Table 6. SSRT crack growth rate in 325ºC PWR primary water.

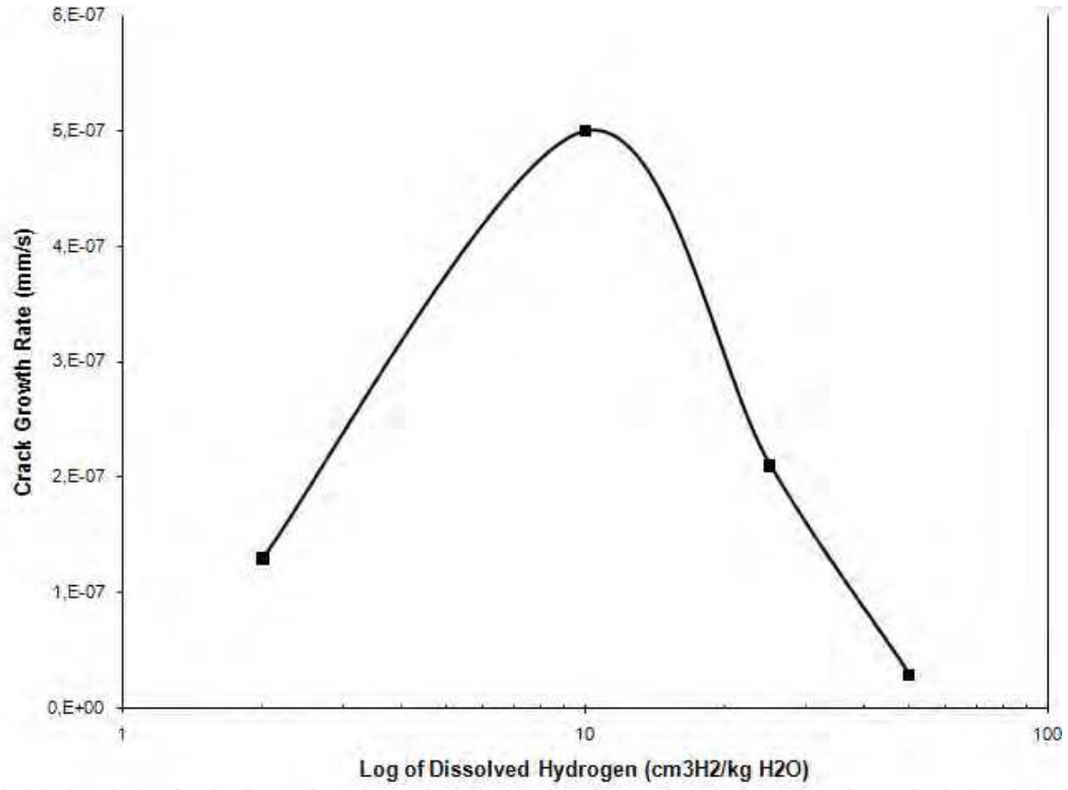

Fig. 19. Relationship between dissolved hydrogen and crack growth rate for Alloy 182 weld in a PWR primary water with obtained for concentrations of 2, 10, 25 and 50 cm^3 H_2 (STP).kg^{-1} H_2O at 325ºC.

It is observed that there is a maximum of the crack growth rate (CGR) plot at 10 cm^3 H_2 (STP).kg^{-1} H_2O and that this CGR maximum is 17 times higher than at 50 cm^3 H_2 (STP).kg^{-1} H_2O. The present results are consistent with the $\Delta ECP_{Ni/NiO}$ values obtained in this work. It was observed that at 10 cm^3 H_2 (STP).kg^{-1} H_2O the potential measured is near Ni/NiO phase transition, also indicating a higher susceptibility to SCC. While at 50 cm^3 H_2 (STP).kg^{-1} H_2O the potential measured is well into the nickel metal regime, showing lower SCC susceptibility.

The present results suggest that in the normal range for operating PWRs (25–50 cm^3 H_2 (STP).kg^{-1} H_2O) the influence of hydrogen content on SCC was important. The crack growth rate at 25 cm^3 H_2 (STP).kg^{-1} H_2O was 7 times higher than at 50 cm^3 H_2 (STP).kg^{-1} H_2O. This result is consistent with that reported by Andresen et al., and Moshier, Paraventi for this range of hydrogen level (Andresen et al., 2009, Moshier & Pavarenti, 2005).

Although the crack growth rates obtained in this work have been the result of testing and evaluating the susceptibility to SCC using the technique of SSRT, They are in agreement with studies by Andresen et al., Moshier, Paraventi, and Dozaki et al. (Andresen et al., 2008, Moshier & Pavarenti, 2005, Dozaki, et al., 2010) who used the constant load test (which require a period of time of about six months to be performed).

3. Conclusion

In the present study, a DMW with alloy 182 was made to reproduce a weld joint of a PWR pressurizer nozzle. The susceptibility of Alloy 182 weld to SCC in PWR primary water was studied in four levels of DH, 2, 10, 25 and 50 cm^3 H_2 (STP).kg^{-1} H_2O. From this study the following remarks can be made:

The OCP measurements enabled the quantification of the location of the nickel/nickel oxide (Ni/NiO) phase transition line for the Alloy 182 weld metal in PWR primary water at temperature of 325ºC. It was observed that the transition Ni/NiO occurs at potentials close to -740 mV.

Whereas the influence of dissolved hydrogen in the Alloy 182 weld susceptibility to SCC can be described by the extent that the corrosion potential deviates from of the potential that corresponding to the transition of Ni/NiO ($\Delta ECP_{Ni/NiO}$) results indicated that a greater resistance of this material to SCC occurs at 50 cm^3 H_2 (STP).kg^{-1} H_2O, followed by 2, 25 and 10 cm^3 H_2 (STP).kg^{-1} H_2O.

The methodology developed using The SSRT test in assessing the Alloy 182 weld SCC susceptibility reproduced the same order of magnitude of the results obtained in constant load test, demonstrating its feasibility for obtained the CGR of this alloy in PWR primary water in less time and cost.

Within the normal range for operating PWRs (25–50 cm^3 H_2 (STP).kg^{-1} H_2O) the influence of hydrogen content on SCC was significant. The crack growth rate at 25 cm^3 H_2 (STP).kg^{-1} H_2O was 7 times higher than at 50 cm^3 H_2 (STP).kg^{-1} H_2O. It is well known from literature data that the stability of oxides formed on nickel-based alloys at high temperature water is influenced by the closeness to the Ni/NiO transition line. In this study it was observed that at 50 cm^3 H_2 (STP).kg^{-1} H_2O the potential is more cathodic and at this condition the measured potential is away from the Ni/NiO phase boundary. These results suggest less SCC susceptibility in DH content of 50 cm^3 H_2 (STP).kg^{-1} H_2O. In view of that, control of dissolved hydrogen can be an effective countermeasure for the mitigation of SCC in PWR primary water.

4. Acknowledgment

The authors would like to thank Fundação de Amparo à Pesquisa do Estado de Minas Gerais (FAPEMIG), Financiadora de Estudos e Projetos (FINEP), Eletronuclear-Eletrobrás

Termonuclear S.A. and Coordenação de Aperfeiçoamento de Pessoal de Nível Superior (CAPES) for the financial support. They also thank Dr. Rik-Wouter Bosch from SCK-CEN for his help during the performance of electrochemical tests at high temperature.

5. References

Aguilar, J. L, Albarran, L. Martinez & Lopez, H. F. (2003). Effect of Grain Boundary Chemistry on the Intergranular Stress Corrosion Cracking Resistance of Alloy 600 in High Purity Water. *Proceedings of Corrosion 2003 Conference & Expo*, No 03539. San Diego, Ca, March, 2003.

Amzallag, C. J. Boursier, M. C. & Gimond, C. (2002). Stress Corrosion Life Experience of 182 and 82 Welds in French PWRS. *Proceedings Fontevraud 5 th International Symposium*, France September, 2002.

Andresen, P. L.; Emigh, Paul. W. & Morra, Martin. M. (2005). Effects of PWR Primary Chemistry and Deaerated Water on SCC. *Proceedings of Corrosion 2005 Conference & Expo*, No 05592. Houston, Texas, April, 2005.

Andresen, P. L. & Hickilng, J. (2007). Effects of B/Li/pH on CST Growth Rates in Ni-Base Alloys. Materials Reliability Program: (MRP 217), EPRI, Palo Alto, CA: 1015008.

Andresen, P. L.; Young, L. M.; Emigh, Paul. W & Horn. Ron. M. (2002). Stress Corrosion Crack Growth Rate Behavior of Ni Alloys 182 and 600 in High Temperature Water. *Proceedings of Corrosion 2005 Conference & Expo*, No 02510. Denver, Co, April, 2002.

Andresen, P. L.; Hickling, J.; Ahluwalia, A. & J. Wilson. (2008). Effects of Hydrogen on SCC Growth Rate of nickel Alloys in high temperature water. *Corrosion*, Vol. 64, No 9, (September, 2008), pp. (707-720). ISSN 0010-9312.

Andresen, P. L.; Hickling, J.; Ahluwalia, A. & J. Wilson. (2009). Effect of Dissolved Hydrogen on Stress Corrosion Cracking of Nickel Alloys and Weld Metals. *Proceedings of Corrosion 2009 Conference & Expo*, No 09414. Atlanta, GA, March, 2009.

ASM Handbook. (1992). Corrosion in the nuclear power industry. Vol. 13. (Materials Park, OH: ASM International, pp. (927). ISBN 087-170-019-0.

ASM Handbook. (2006). Corrosion Environment and Industries. Vol. 13 C (Materials Park, OH: ASM International, pp. (362-385). ISBN 978-0-87170-709-3.

ASME – American Society of Mechanical Engineers (2004). Boiler and Pressure Vessel Code – Section IX, Welding and Brazing Qualification, 2004. ISBN 079-182-894-8.

ASTM E8. (2000a). Standard Test Methods for Tension Testing of Metallic Materials. In: *Annual book of ASTM Standards. West Conshohocken*, PA: ASTM, 2000a.

ASTM G 129. (1995). Standard Test Methods for Slow Strain Rate Testing to Evaluate the Susceptibility of Metallic Materials to Environmentally Assisted Cracking. In: *Annual book of ASTM Standards*. West Conshohocken, PA: ASTM, 1995.

ASTM G 49. (2000b). Standard Test Methods for Preparation and Use of Direct Tension Stress-Corrosion Test Specimens. In: *Annual book of ASTM Standards*. West Conshohocken, PA: ASTM, 2000b.

Attanasio, S. A. & Morton, D. S. (2003) Measurement of the Nickel Oxide Transition in Ni-Cr-Fe Alloys and Updated Data and Correlations to Quantify the Effect of Aqueous Hydrogen on Primary Water SCC. *Proceedings 11th Int. Conf. Environmental Degradation of Materials in Nuclear Power Systems*, Stevenson, WA, August, 2003.

Alexandreanu, B.; et al. (2007). Environmentally Assisted Cracking in Light Water Reactors. *Argone National Laboratory Annual Report*, NUREG/CR-4667, March, 2007.

Banford, W. & Hall, J. (2003) A Review of Alloy 600 Cracking in Operating Nuclear Plants: Historical Experience and Future Trends. *Proceedings 11th Int. Conf. Environmental Degradation of Materials in Nuclear Power Systems*, Stevenson, WA, August, 2003.

Bosch, R-W.; et al. (2003). LIRES: A European Sponsored Research Project to Develop Light Water Reactor Reference Electrodes. *Proceedings 11th Int. Conf. Environmental Degradation of Materials in Nuclear Power Systems*, Stevenson, WA, August, 2003.

Brown, C. M. & Mills, W. J. (2003). Stress Corrosion Crack Growth Rates for Alloy 82H Welds in High Temperature Water. *Proceedings 11th Int. Conf. Environmental Degradation of Materials in Nuclear Power Systems*, Stevenson, WA, August, 2003.

Davis, J. R. (2006). Hardfacing, Weld Cladding, and Dissimilar Metal Joining. In: *ASM Handbook – Welding, Brazing and Soldering*, Vol. 6, pp. (2044-2061), ISBN 87170-377-7.

Dozaki, K; et al. (2010). Effects of Dissolved Hydrogen Content in PWR Primary Water on PWSCC Initiation Property. *E-Journal of Advanced Maintenance.* Vol. 2, (August, 2010), pp. (65-76). ISSN 1883-9894.

White, G. A. (2004). Crack Growth Rates for Evaluating PWSCC of Alloy 82, 182 and 132 Welds Materials Reliability Program: Materials Reliability Program: (MRP-115). EPRI, Palo Alto, CA: 1006696.

Fallatah, M. G.; Sheikh, K. A.; Khan, Z. & Boah, K. J. (2002). Reliability of Dissimilar Metal Welds subjected to Sulfide Stress Cracking. KFUPM - King Fahd University of Petroleum & Minerals. *Proceedings of 6th Saudi Engineering Conference*, Dhahran, Saudi Arabia, December, Vol. 5, pp. (297-312).

Fukumura, T. & Totsuka, N. (2010). PWSCC Susceptibility of Stainless Steel and Nickel Based Alloy of Dissimilar Metal Butt Welds. *Proceedings of Corrosion 2005 Conference & Expo*, No 10245. San Antonio, TX, March, 2010.

Garbett, K.; Henshaw, J. & Sims, H. E. (2000). Hydrogen and Oxygen Behaviour in PWR Primary Coolant. *International Conference of Water Chemistry of Nuclear Reactor System 8*. ISBN 0727729586. *British Nuclear Energy Society*. Vol. 1, 2000.

Giannuzzi, A.; Hermann, R. & Smith, R. (2004). Recommendations for Testing of Emerging Mitigation Techniques for PWSCC. Materials Reliability Program: (MRP-119). EPRI, Palo Alto, CA: 1009501.

Gomez-Briceño, D. & Serrano, M. (2005). Aleaciones Base Niquel em Condiciones de Primario de Los Reactores Tipo PWR. *Nuclear España: Revista de la Sociedad Nuclear Española*, No. 250, (March, 2005), pp. (17-22), ISSN 1137-2885.

Gorman, J.; Hunt, S.; Pete, R. & White, G. A. (2009). PWR Reactor Vessel Alloy 600 Issues. In: *ASME –American Society of Mechanical Engineering*.

IAEA - International Atomic Energy Agency. (2003). Assesment and Management of Ageing of Major Nuclear Power Plant Components Important to Safety - Primary Piping in PWRs. IAEA – TECDOC 1361, 2003.

Jang, C.; Lee. J.; Kim, S. J. & Jim, E. T. (2008). Mechanical Property Variation Within Inconel 82/182 Dissimilar Metal Weld Between Low Alloy Steel and 316 Stainless Steel. *International Journal of Pressure Vessels and Piping*, Vol. 85, No. 9, (September, 2008), pp. (635-646), ISSN 0308-0161.

King, C. (2005). Primary System Piping Butt Weld Inspection and Evaluation Guidelines Materials Reliability Program: (MRP-139), Eletric Power Research Institute – EPRI, Palo Alto, 2005, CA: 1010087.

Kou, S. (2003). Welding Metallurgy. Second Edition, John-Wiley & Sons, ISBN 0-471-43491-4.

Lima, L. I. L; Schvartzman, M. M. A. M, Figueiredo, C. A. & Bracarense, A. Q. (2011). Stress Corrosion Cracking Behavior of Alloy 182 Weld in Pressurized Water Reactor Primary Water Environment at 325ºC. *Corrosion,* Vol. 65, No 085004, (August, 2011), pp. (1-9), ISSN 0010-9312.

Lu, Z.; Takeda, Y. & Shoji, T. (2008). Some Fundamental Aspects of Thermally Activated Process Involved in Stress Corrosion Cracking in High Temperature Aqueous Environments. *Journal of Nuclear Materials,* No. 383, pp. (92–96), ISSN 0022-3115.

Miteva, R & Tayllor, N. G. (2006). General Review of Dissimilar Metal Welds in Piping Systems of Pressurized Water Reactors, Including WWER Designs. *European Comission DG-JRC/IE, Petten*, Netherlands, EUR 22469 EN, 2006.

Morton, D. S.; Attanasio, A. S.; Fish, S. J. & Schurman, K. M. (1999). Influence of Dissolved Hydrogen on Nickel Alloys Stress Corrosion Cracking in High Temperature Water. *Proceedings of Corrosion 1999 Conference & Expo*, No 99447, San Antonio, Texas, April, 1999.

Morton, D. S; Attanasio, S. A. & Young, G. A. (2001). Primary Water SCC Understanding and Characterization Through Fundamental Testing in the Vicinity of the Nickel/Nickel Oxide Phase Transition. LM_01K038.

Nishikawa, Y.; Totsuka, N. & Arioka, K. (2004). Influence of Temperature on PWSCC Initiation and Crack Growth Rate Susceptibility of Alloy 600 Weld Metals. *Proceedings of Corrosion 2004 Conference & Expo,* No 04670, New Orleans, Lousiana, March, 2004.

NACE TMO19 (2004). Slow Strain Rate Test Method for Screening Corrosion Resistant Alloys (CRAs) for Stress Corrosion Cracking in Sour Oifield Service. Houston, TX: Nace, 2004.

Pathania, R. S., Mcilree, R. R. & Hickling, J. (2002). Overview of CST of Alloys 182/82 in PWRs. *Proceedings Fontevraud 5 th International Symposium*, France September, 2002.

Paraventi, D. J. & Moshier, W. C. (2005). The Effect of Cold Work and Dissolved Hydrogen in the Stress Corrosion Cracking of Alloy 82 and Alloy 182 Weld Metal. *Proceedings of 12th International Conference Environmental Degradation of Materials in Nuclear Systems*, Salt Lake City, Utah, August, 2005.

Peng, Q. J., Shoji, T., Yamauchi, H. & Takeda, Y. (2007). Intergranular Environmentally Assisted Cracking of Alloy 182 Weld Metal in Simulated Normal Water Chemistry of Boiling Water Reactor. *Corrosion Science*, No. 49, (January, 2007) pp. (2767-2780), INSS 0010-938X.

Rebak, R. B & Hua, F. H. (2004). The Role of Hydrogen and Creep in Intergranular Stress Corrosion Cracking of Alloy 600 and Alloy 690 in PWR Primary Water Environments - a Review. In: *Environment-Induced Cracking of Materials – Chemistry, Mechanics and Mechanisms*, Sergei A. Shipilov, Russel H. Jones, Jean Marc Olive, Raúl B. Rebak, Elsevier, ISBN 9780080446356.

Rebak, R. B & Szklarska-Smialowska, Z. (1996). The Mechanism of Stress Corrosion Cracking of Alloy 600 in High Temperature Water. *Corrosion Science*, No. 6, (June, 1996), pp. (971 – 988) INSS 0010-938X.

Rebak, R. B, Xia, Z & Szklarska-Smialowska, Z (1993). Effects of Carbides on Susceptibility of Alloy 600 to Stress Corrosion Cracking in High-Temperature Water. *Corrosion*, Vol. 49, No 11, (November, 1993), pp. (1-10), ISSN 0010-9312.

Schaefer, A. (1979). Dissimilar Metal Weld Failure Problems in Large Steam Generators. *Power*, pp. (68 – 69), 1979.

Scott, P. M. (2004). An Overview of Materials Degradation by Stress Corrosion in PWRs. Proceedings of Eurocorr- Annual European Corrosion Conference of the European Federation of Corrosion, ISBN 295168441X, Nice, Acropolis, September, 2004.

Scott, P.M. & Meunier, M. -C. (2007). Review of Stress Corrosion Cracking of Alloys 182 and 82 in PWR Primary Water Service, Materials Reliability Program: (MRP-220), Eletric Power Research Institute – EPRI, Palo Alto, 2007, CA: 1015427.

Schvartzman, M. M. A. M.; Quinan, M. A.; Campos, W. R. C. & Lima, L. I. L. (2009). Avaliação da suscetibilidade à corrosão sob tensão da ZAC do aço inoxidável AISI 316L em ambiente de reator nuclear PWR. *Soldagem & Inspeção,* Vol 14, No 3, (Julho/Setembro, 2009). ISSN 0104-9224.

Sedricks, A. J. (1990). Stress Corrosion Cracking Test Methods. In: *Corrosion Testing Made Easy; Stress Corrosion Cracking Testing Methods*, B.C. Syrett, NACE. ISBN 091-556-740-7.

Seifert, H. P.; et al. (2008). Environmentally Assisted Cracking Behavior in the Transition Region of an Alloy 182/SA 508 Cl.2 Dissimilar Metal Weld Joint in Simulated Boiling Water Reactor Normal Water Chemistry Environment. *Journal of Nuclear Materials*, Vol. 378, pp. (197-290), ISSN 022-3115.

Speidel, M. O. & Magdowski, R (2000). Stress Corrosion Crack Growth in Alloy 600 Exposed to PWR and BWR Environments. *Proceedings of Corrosion 2000 Conference & Expo*, No 00222, Orlando, Fl, April, 2000.

Takiguchi, H.; Ullberg, M. & Uchida, S. (2004). Optimization of Dissolved Hydrogen Concentration for Control of Primary Coolant Radiolysis in Pressurized Water Reactors. *Journal of Nuclear Science and Technology*, Vol. 41, No. 5, pp. (601–609), (May, 2004). ISSN 022-3131.

Totsuka, N.; Sakai, S.; Nakajima, N. & Mitsuda, H. (2000). Influence of Dissolved Hydrogen on Primary Water Stress Corrosion Cracking of Mill Annealed Alloy 600. *Proceedings of Corrosion 2000 Conference & Expo*, No 00212, Orlando, Fl, April, 2000.

Totsuka, N.; Nishikawa, Y. & Nakajima, N. (2002). Influence of Dissolved Hydrogen and Temperature Primary Water Stress Corrosion Cracking of Mill Annealed Alloy 600. *Proceedings of Corrosion 2002 Conference & Expo*, No 02523, Denver, Co April, 2002.

Totsuka, N.; Nishikawa, Y.; Kaneshima, Y. & Arioka, K. (2003). The Effect of Strain Rate on PWSCC Fracture Mode of Alloy 600(UNS N06600) and 304 Stainless Steel (UNS S30400). *Proceedings of Corrosion 2003 Conference & Expo,* No 03538, San Diego, Ca, March, 2003.

Tsai, W.T.; Yu, C.L. & Lee, J. I. (2005). Effect of Heat Treatment on the Sensitization of Alloy 182 Weld. *Scripta Materialia*, No. 53, pp. (505–509), ISSN 1359-6462.

White, G. A.; Nordmann, N. S.; Hickling, J. & Harrington, C. D. (2005). Development of Crack Growth Rate Disposition Curves for Primary Water Stress Corrosion Cracking (PWSCC) of Alloy 82,182 and 132 Weldments. *Proceedings of 12th International Conference Environmental Degradation of Materials in Nuclear Systems*, Salt Lake City, Utah, August, 2005.

IntechOpen

IntechOpen

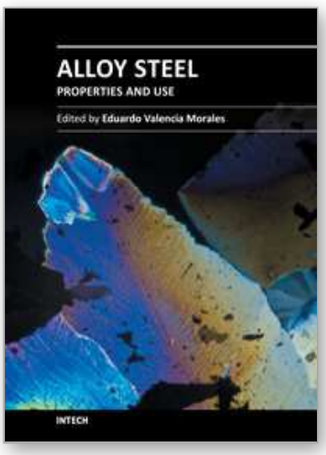

Alloy Steel - Properties and Use

Edited by Dr. Eduardo Valencia Morales

ISBN 978-953-307-484-9
Hard cover, 270 pages
Publisher InTech
Published online 22, December, 2011
Published in print edition December, 2011

The sections in this book are devoted to new approaches and usages of stainless steels, the influence of the environments on the behavior of certain classes of steels, new structural concepts to understand some fatigue processes, new insight on strengthening mechanisms, and toughness in microalloyed steels. The kinetics during tempering in low-alloy steels is also discussed through a new set-up that uses a modified Avrami formalism.

How to reference

In order to correctly reference this scholarly work, feel free to copy and paste the following:

Luciana Iglésias Lourenço Lima, Mônica Maria de Abreu Mendonça Schvartzman, Marco Antônio Dutra Quinan, Célia de Araújo Figueiredo and Wagner Reis da Costa Campos (2011). Influence of Dissolved Hydrogen on Stress Corrosion Cracking Susceptibility of Nickel Based Weld Alloy, Alloy Steel - Properties and Use, Dr. Eduardo Valencia Morales (Ed.), ISBN: 978-953-307-484-9, InTech, Available from: http://www.intechopen.com/books/alloy-steel-properties-and-use/influence-of-dissolved-hydrogen-on-stress-corrosion-cracking-susceptibility-of-nickel-based-weld-all

INTECH
open science | open minds

InTech Europe
University Campus STeP Ri
Slavka Krautzeka 83/A
51000 Rijeka, Croatia
Phone: +385 (51) 770 447
Fax: +385 (51) 686 166
www.intechopen.com

InTech China
Unit 405, Office Block, Hotel Equatorial Shanghai
No.65, Yan An Road (West), Shanghai, 200040, China
中国上海市延安西路65号上海国际贵都大饭店办公楼405单元
Phone: +86-21-62489820
Fax: +86-21-62489821

© 2011 The Author(s). Licensee IntechOpen. This is an open access article distributed under the terms of the Creative Commons Attribution 3.0 License, which permits unrestricted use, distribution, and reproduction in any medium, provided the original work is properly cited.

IntechOpen

IntechOpen